

Structure and function of the vertebrate magnetic sense

Michael M. Walker*, Carol E. Diebel*, Cordula V. Haugh*, Patricia M. Pankhurst*†, John C. Montgomery* & Colin R. Green‡

* Experimental Biology Research Group, School of Biological Sciences, University of Auckland, Private Bag 92019, Auckland, New Zealand

‡ Department of Anatomy with Radiology, School of Medicine, University of Auckland, Private Bag 92019, Auckland, New Zealand

Some vertebrates can navigate over long distances using the Earth's magnetic field, but the sensory system that they use to do so has remained a mystery. Here we describe the key components of a magnetic sense underpinning this navigational ability in a single species, the rainbow trout (*Oncorhynchus mykiss*). We report behavioural and electrophysiological responses to magnetic fields and identify an area in the nose of the trout where candidate magnetoreceptor cells are located. We have tracked the sensory pathway from these newly identified candidate magnetoreceptor cells to the brain and associated the system with a learned response to magnetic fields.

The use of the Earth's magnetic field by animals for navigation during migration and homing has been studied intensively¹ but the detection mechanism and the sensory pathway between the detector and the brain that underpin navigation behaviour remain unknown. Hypotheses have been proposed that link the detection of magnetic fields to vision, electroreception and magnetite particles^{2–6}. Magnetic detection mechanisms mediated through the visual system^{2,3} seem to be contradicted by the ability of salmon, turtles and lobsters to orientate magnetically in total darkness^{7–9}. Similarly, electrical induction could mediate magnetoreception by elasmobranchs⁴ but not by species that do not detect electrical fields. Magnetoreception using magnetite particles^{5,6} could readily permit the known responses to magnetic field stimuli^{10,11} and is supported by impairment¹² and pulse magnetization^{13,14} experiments. But magnetite-based magnetoreceptors have not yet been found in any animal. Thus, each of these detection mechanisms has so far failed at some level to provide a convincing description of how animals detect magnetic fields.

Identifying and describing the components of the magnetic sensory system presents several challenges. First, magnetic fields are relatively simple stimuli with only two dimensions—direction and intensity—which vary slowly in space and time. Hence, large numbers of sensory cells, corresponding large numbers of sensory nerves and complex central processing centres are not necessary for magnetic field detection. Second, animals only respond to magnetic fields if they are actively moving or attempting to move¹⁵, which makes it difficult to elicit powerful behavioural responses to magnetic fields in most laboratory situations. Third, tissues are transparent to magnetic fields, making accessory sensory structures such as lenses that focus the stimuli on receptor cells unnecessary. Receptor cells could be dispersed throughout an organism. Finally, single-domain magnetite particles suitable for use in magnetoreception¹⁰ would be too small (≤ 100 nm) for detection by conventional light microscopy and too rare (≤ 5 p.p.b. by volume) for detection by conventional transmission electron microscopy (TEM). It should therefore come as no surprise that standard behavioural, physiological and anatomical approaches to the study of sensory systems have been difficult to apply to the magnetic sense.

We have now recorded behavioural and electrophysiological responses to magnetic fields and identified candidate receptor cells in the trout. We have used a discrimination training

procedure¹⁶ to demonstrate robust behavioural responses by the trout to the presence and absence of a magnetic field anomaly in experimental tanks. We have identified single neurons in the superficial ophthalmic ramus (ros V) of the trigeminal nerve that respond to changes in the intensity but not the direction of an imposed magnetic field, and used a combination of new imaging and microscopic techniques to identify candidate magnetite-based magnetoreceptor cells in the nose of the trout. The cells contain crystals that are iron-rich and almost identical in form to single-domain magnetite crystals previously extracted from sockeye salmon¹⁷. We have also traced fine branches of the ros V nerve to the same cellular layer (the lamina propria within the olfactory lamellae) as the candidate magnetoreceptor cells. Identification of the critical components of the magnetic sense brings a new perspective to the study of long-distance orientation in a variety of vertebrate groups.

Learned magnetic discrimination

Our experiments exploited previous findings that magnetic discrimination training is successful when the subjects must move to sample spatial patterns in intensity of the magnetic field^{18–20} but fails when the experimental stimuli differ only in direction^{1,18,21,22}. We trained three juvenile rainbow trout individually to swim to and strike repeatedly at a target to obtain food (Fig. 1a). Our measure of magnetic stimulus discrimination was therefore the rate at which the fish struck the target in anticipation of reinforcement with food or lack of reinforcement at the end of each trial¹⁶. The magnetic stimuli to be discriminated were the presence and absence of a magnetic intensity anomaly focused on the target and superimposed on the background of the Earth's magnetic field.

A clear difference in response rates developed after the third training session (Fig. 1b) with the fish responding at a consistently higher rate to the reinforced stimulus (S+) than to the non-reinforced stimulus (S–). The difference between the average response rates to S+ and S– was statistically reliable (ANOVA: $F_{1,2}$ stimuli = 25.9281, $P = 0.0365$). The response to S– was more variable in individual fish than the response to S+ ($F_{2,4}$ subjects = 19.2265, $P = 0.0086$). There seemed to be no difference if the magnetic anomaly was the reinforced or non-reinforced stimulus as the graphs for individual fish were all similar to Fig. 1b. The separation of response rates to S+ and S– with time during the experiments was confirmed statistically ($F_{14,192}$ subjects \times stimuli \times sessions = 9.64375, $P = 0.0403$). The likely cause of this effect is an interaction between the development of discrimination (response rates to S+ and S– changed with time

† Present address: Department of Aquaculture, University of Tasmania at Launceston, Box 1214 Launceston, Tasmania 7250, Australia.

during the experiment) and variability of behaviour among the subjects.

Our results are consistent with the idea that animals learn most readily to discriminate magnetic fields when the conditioned response requires movement and when the fields are spatially distinctive. Yellowfin tuna, honeybees and now rainbow trout all readily discriminated magnetic fields under these conditions but the tuna and honeybees both failed to discriminate when one of these conditions was not met^{18,20}. Despite these constraints, however, magnetic discrimination by the trout can now be analysed in the same ways as discrimination of other stimuli by other species (for example, ref. 16).

Neural responses to magnetic field intensity

We recorded from sensory nerves and areas of the brain that receive neural input from the anterior skull, where magnetite had previously been found^{17,23}. The only positive responses were found in the rosl V nerve. The nerve runs in close association with the superficial ophthalmic ramus of the dorsal anterior lateral-line nerve (rosl) above the eye. The two rami form the supra-orbital trunk (SOT; ref. 24). These rami separate after passing through the orbit and innervate the snout area of the head.

We used a series of search stimuli presented as uniform square waves that changed direction, intensity, or both direction and intensity of the magnetic field (represented by *B* in Fig. 2) around the head of experimental fish. The stimuli were produced by subtracting, adding and switching between subtracting and adding 50 microTesla (μT) to the background field (25 μT ; see Methods) in the experimental tank. For the first search stimulus (designated SS1), subtracting 50 μT reversed the magnetic field direction in the tank (represented by *B*: $-B$ for onsets and $-B$:*B* for offsets in Fig. 2) but did not change intensity. In contrast, adding 50 μT (SS2) trebled the intensity without changing field direction in the tank (represented by *B*:3*B* for onsets, 3*B*:*B* for offsets in Fig. 2). Our third stimulus (SS3) combined these stimuli by reversing the polarity of the input current to the coils rather than switching it off. The field in the situation was thus switched between a field with the same intensity but reversed direction relative to the background field and a field with the same direction but three times the intensity of the background field ($-B$:3*B* for onsets; 3*B*: $-B$ for offsets in Fig. 2).

The square-wave stimuli induced transient voltage-gradient artefacts of 1.4 V cm^{-1} in 50% sea water that could potentially affect the activity of the nerves being recorded. The artefacts were, however, mirror images of each other when current polarities were reversed. That is, the artefact caused by the onset of SS2 was identical to the artefact caused by the offset of SS1, and vice versa. Response to the onset, for example, of SS2 but not to the offset of SS1 would therefore distinguish between response to the magnetic stimulus and response to the associated artefact.

We located two populations of spontaneously active neurons in the rosl V nerve (Fig. 2a). The 'fast' population showed high-amplitude signals ($>7.5\text{ mV}$ above background in extracellular recordings) and high firing rates (mean 39 Hz). The 'slow' population showed low-amplitude signals (1–2 mV above background) and low firing rates (mean 20 Hz) that were significantly lower than for the fast units ($t_s = 3.2, P < 0.01$ for the firing rates of the units shown in Fig. 2a). None of the fast units ever responded to magnetic stimuli, whereas a small proportion of the slower units responded to magnetic stimuli with excitatory responses to the onset of SS2 (Fig. 2c–e) as well as both excitatory and inhibitory responses to the onsets and offsets of SS3 (Fig. 2f).

The responsive units showed regular firing patterns, as seen by the normally distributed intervals between spikes (Fig. 2b), except during the transient responses to SS2 and SS3. To our surprise, no unit responded to SS1, nor was there any off-response corresponding to the excitatory on-responses to SS2 and SS3 (Fig. 2d). Response to SS2 presented at 0.5 and 1 Hz by two of the units is

shown in Fig. 2e. The latency and time-course (the first point after the stimulus step and the period during which the firing rate was more than two standard deviations above the mean for each unit) of the responses by the two units exposed to both stimulation frequencies were similar but the peak amplitudes of the responses increased and decreased, respectively, when the rate at which SS2 was presented increased from 0.5 to 1 Hz (Fig. 2e).

Five units responded to SS3 (of 43 slow units tested with this stimulus). Three units responded to the step where intensity increased from $-B$ to 3*B* and one responded to the step where the intensity decreased from 3*B* to $-B$ (Fig. 2f). Both response latencies and durations for these units ranged between 15 and 80 ms, with peak amplitudes of response ranging between 4.8 and 16.8 times the background firing rate for units exhibiting excitation. The firing rate of the fifth unit that responded to SS3 was nearly halved for about 40 ms after the onset of SS3 (mean \pm s.d. firing rates in post-stimulus time histograms: 4–42 ms after stimulus onset, $25.2 \pm 17.4\text{ Hz}$; 43–442 ms after stimulus onset, $36.3 \pm 25.0\text{ Hz}$; $t_s = 2.7, P < 0.01$).

Although the responses by units in the rosl V to magnetic field intensity are consistent with the behavioural responses in the trout, it is important to exclude other explanations for our electrophysiological data. The failure of the units in the rosl V that responded to SS2 to respond to SS1 (*B*: $-B$ and $-B$:*B* in Fig. 2d) counters the possible arguments that the units responded either to changes in magnetic field direction that were too small for us to detect or to electrical or mechanical artefacts induced by SS2 (*B*:3*B* and 3*B*:*B*)

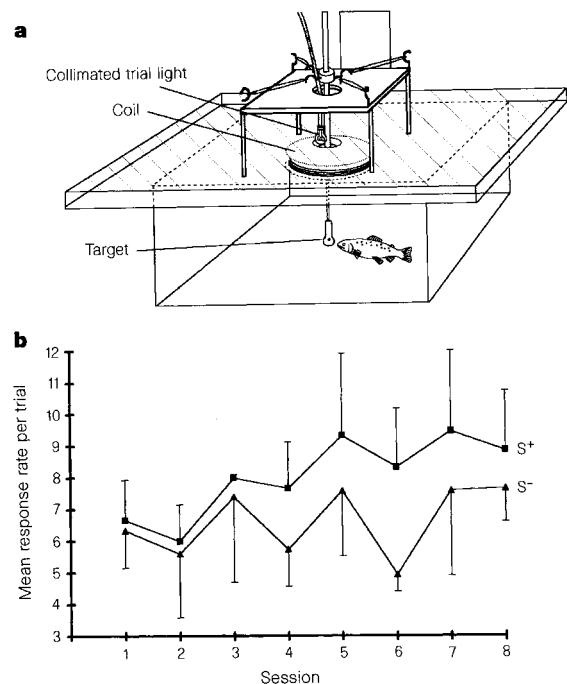


Figure 1 Discrimination of the presence and absence of a magnetic anomaly by rainbow trout. **a**, A 50-turn coil (4 cm diameter) induced a narrowly localized magnetic field anomaly (peak intensity 70 μT) which, when added to the local background field (55 μT), produced a peak intensity of 125 μT at the water surface directly below the axis of the coil. A response bar, tipped with a teflon target and aligned with the axis of the coil, projected just below the water surface at the centre of the tank. Liquid fish-food pumped through the bar and delivered at the target permitted a close association of stimulation, response and reinforcement. The experimental procedures were fully automated. **b**, Magnetic discrimination data presented as the mean response rate per trial by the three fish with the data blocked over the five S+ and S- trials given in balanced quasi-random order in each training session. Vertical lines indicate s.e.m.

because all such artefacts were equivalent in both search stimuli. Conversely, the failure of the units that responded to SS2 to respond to SS1 does not rule out the existence of units that would respond to SS1.

Candidate magnetoreceptor cells

Demonstrating a magnetite-based detection mechanism depends first on the identification of magnetite associated with candidate magnetoreceptor cells. Detecting single-domain magnetite *in situ* is difficult because of the small size of the crystals and their very low volume concentrations in tissues. We have partly resolved the detection problem in large volumes of tissue by using the confocal laser scanning microscope (CLSM) in reflection mode to render chains of single-domain magnetite visible at the light microscope level. The chains of magnetite discovered in magnetotactic bacteria²⁵ reflect the laser light to produce bright spots which are clearly associated with the bacterial cells when viewed in transmitted light (Fig. 3a). A search through rainbow trout heads embedded in both JB4 and Epon resins using CLSM revealed crystalline material in the lamina propria layer within olfactory lamellae. These crystals gave reflections of similar intensity and dimensions to the magnetite in the bacteria (Fig. 3b). The lamina propria is the layer separating the columnar epithelial folds that make up each lamella. It is separated from the olfactory epithelial layer by a basal lamina. Serial thin sections through one of the reflections in the lamina propria revealed the crystal (arrows) shown in Fig. 3c in bright-field (left) and dark-field (centre) TEM. Further TEM analysis showed that the

crystal was iron-rich (Fig. 3d) and almost identical in size (length 50 nm) and shape to single-domain magnetite extracted from sockeye salmon¹⁷.

The cells containing the reflecting particles are 10–12 μm in length, have a distinctive tri-lobed shape and are consistently located near the basal lamina of the olfactory epithelium. Cells containing reflections are relatively rare, with never more than two or three being detected at a time within the volume (roughly 150 μm^3) sampled by the CLSM at the magnification required to detect the reflections. In addition, the spots produced by the crystals in the olfactory epithelium were punctate in both the horizontal and vertical dimensions. We detected reflections in other regions of the trout head but these could be excluded as possible sites for the magnetoreceptors. Reflections associated with bone in the head of the trout were easily detectable at low magnification in CLSM and differed in appearance and dimensions from the reflections produced by magnetite in the bacteria. In contrast, reflections from the pigment melanin could be excluded on the basis of their clear association with pigment cells, which are large and have a distinctive stellate morphology.

The similarity of the reflectances in the trout to magnetite reflectances in the bacteria, and their consistent location near the basal lamina of the olfactory epithelium of the trout, lead us to view the reflectance-containing cells as candidate magnetoreceptors. We are encouraged that the crystal shown in Fig. 3 was similar in size, shape and presence of iron to magnetite extracted from sockeye salmon¹⁷. The crystal is likely to be part of a larger group such as a

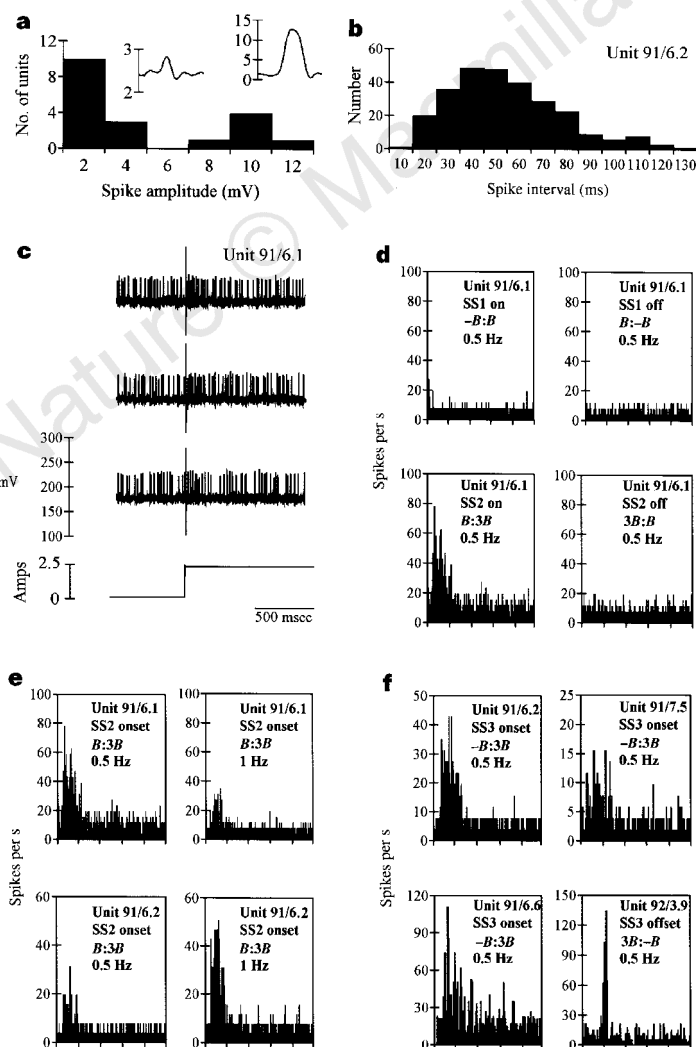


Figure 2 Electrophysiological responses to magnetic fields. **a**, Histogram of spike amplitudes for 19 units recorded as they were encountered in the ros V of the rainbow trout. We divided the units recorded into two populations on the basis of spike amplitudes (illustrated in the inset plots of single spikes representing each population). Mean firing rates \pm s.d. for the two populations of units were $20 \pm 10.3\text{Hz}$ and $39 \pm 14.9\text{Hz}$. Responsive units were found only in the population of units with low spike amplitudes and firing rates. Ordinates in mV for inset plots of single spikes. **b**, Histogram of spike intervals in the absence of experimental stimulation for the unit 91/6.2 (one of the responsive units shown in **e**; 286 spike intervals recorded). The median spike interval for the unit is 45 ms. The data are roughly normally distributed, consistent with a regular firing rate of about 20 Hz. **c**, Peristimulus activity of a single unit (91/6.1) in the ros V of the rainbow trout. The onset of SS2 (bottom trace) is aligned with the associated stimulus artefacts in the top three traces (clipped for clarity). To the left of the artefacts, the unit is spontaneously active in the background magnetic field. To the right of the artefacts, the traces show the activity of the unit for 1 s after the onset of SS2. Acceleration of the firing rate of the unit is evident for the first 100 ms after the stimulus step. **d**, Post-stimulus time histograms (PSTHs) of responses by the unit shown in **c** to SS1 and SS2 presented 128 times at 0.5 Hz (on for 1 s then off for 1 s). **e**, PSTHs of responses by two spontaneously active units to the onsets of SS2 presented 128 times at 0.5 and 1 Hz. **f**, PSTHs of responses by four spontaneously active units to SS3. The stimuli were presented 128 times in each case. Each plot in **d–f** begins at the step change in the field and is of duration 500 ms. The magnetic field remained constant throughout the period. Unit identification number, search stimulus number, stimulus step and presentation rates are listed. Sampling bin widths are 2 ms in **d**, **e** and in the upper-left panel of **f** and 4 ms in the remaining panels of **f**. Tick marks on the abscissae are at 100 ms intervals.

chain of crystals, as is the case in the magnetotactic bacteria, because it was too small on its own to produce a reflection that could be detected at the light microscope level.

Association between magnetoreceptors and nerves

If the cells in the lamina propria of the olfactory lamellae do indeed contain magnetite used in magnetoreception, it is reasonable to predict that the magnetically responsive nerve should be linked to the candidate receptor cells. We have used serial histological sections and DiI, a fluorescent lipophilic dye, to trace branches of the ros V from the site where electrophysiological recordings of responses to magnetic field stimulation were made, to the endings of the individual nerve cells (Figs 4–6).

DiI migrated in both anterograde and retrograde directions along myelinated and unmyelinated fibres in the ros V. Posterior to the orbit, it joined other branches of the trigeminal nerve and ended in cell bodies that make up part of the anterior ganglion. From the ganglion, the labelled nerve tracts entered the anterior dorsal area of the medulla oblongata. Anterior to the orbit, the ros V coalesces with the ros I as it passes through a foramen of the neurocranium to the snout region. After leaving the foramen, the ros V separates

again from the ros I and has rami that surround the olfactory nerve, innervate the superficial epidermis of the snout and surround, as well as penetrate, the nasal capsule.

The ros V rami that surround the nasal capsule form a complex network from which very fine processes penetrate the capsule wall and terminate in the lamina propria of the olfactory lamellae. To link these fine processes back to the network, we developed a combination of techniques using CLSM optical slicing, computerized three-dimensional image-stack analysis and reconstruction,

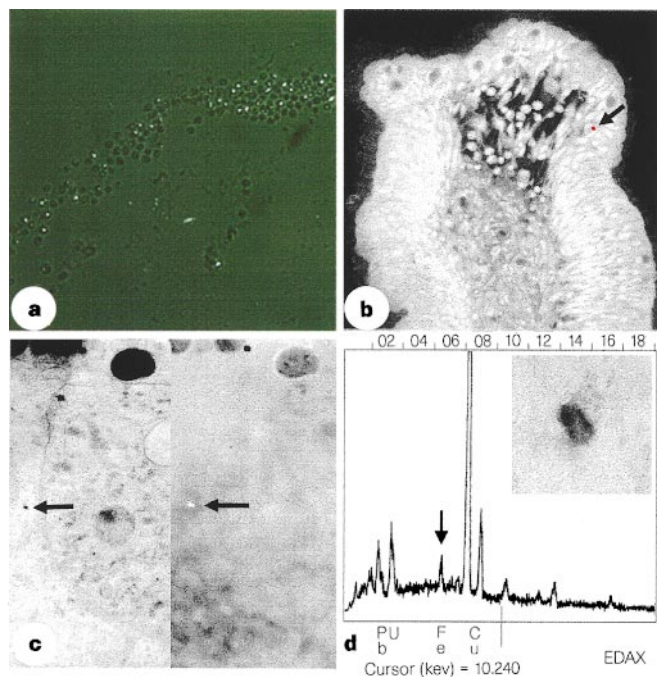


Figure 3 Detection of intracellular magnetite. **a**, Overlaid images of magnetotactic bacteria collected using the method of ref. 37, dried onto a coverslip and viewed using a CLSM in reflected and transmitted light modes. Bright spots observed in reflection mode coincide with the location of the magnetotactic bacteria cells viewed in transmitted light mode (magnification $\times 290$). **b**, A reflectance contained in a cell located near the basal lamina of the olfactory epithelium of the trout has been false-coloured red (arrow) and overlaid onto an autofluorescence image of the olfactory lamella taken at the same depth and magnification ($\times 190$). The lamina propria is the central space that separates the folds of the columnar olfactory mucosa. **c**, Bright-field (left) and dark-field (right) TEM of a crystal associated with a reflectance in the trout olfactory lamellae. In bright-field TEM, both the crystal (arrow) and a much larger pigment granule (top centre) are electron-dense. In dark-field TEM, the crystal (arrow) reflects the electron beam strongly whereas the large pigment granule (upper right) does not (magnification $\times 12,500$). **d**, Energy dispersive analysis of X-ray emissions (EDAX) of the crystal in **c**. Inset shows the crystal (length 50 nm) at higher magnification. The copper (Cu) peak is due to the copper grid used, and lead (Pb) and uranium (U) peaks are from TEM stains. The peak from iron (Fe) present in the crystal is indicated by an arrow. This peak was absent in control regions of the same section.

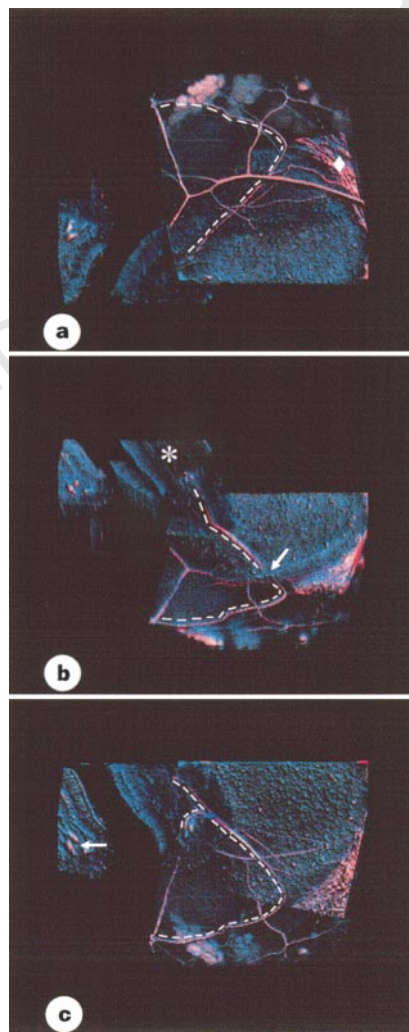


Figure 4 Three steps in a 270° rotation series of a three-dimensional volume-rendered image stack showing the path of a nerve process (right of dashed line) as it enters the top of a lamella. Lipid deposits can be seen on the outside of the nasal membrane (top centre of **a** and bottom centre of the rotated volumes **b** and **c**, and correspond to the yellow layer of Fig. 6c). **a**, The rendered volume rotated 70° from the top shows part of a fine process (right of dashed line) of the ros V as it goes over the outside of the nasal capsule and curves downwards and through the nasal membrane. A representative region of the extensive network that surrounds the outside of the nasal capsule can be best seen to the right of the image (indicated by diamond symbol). **b**, The rendered volume vertically rotated 162° from **a** to show the nasal capsule from within, and the fine process penetrating through the nasal membrane (arrow) from the outside and continuing into a lamella (asterisk). **c**, The rendered volume has been rotated a further 35° and the fine process can be seen to branch within the lamella, one branch curving around the lamellar artery and the other proceeding along towards the lamellar base. The artery is 'U'-shaped at the top of the lamella; its ascending and descending arms are more clearly seen in the lamina propria layer of the lamella on the left (arrow) (magnification $\times 65$).

and volume rotations. After analysing the images individually, we reconstructed areas of the nasal capsule in three dimensions, allowing us to rotate the volumes and definitively trace the fine processes within the lamina propria back to the specific rami of the ros V that surround the nasal capsule (Figs 4, 6).

From these reconstructions, we identified two distinct branching patterns by which the ros V innervates the olfactory lamellae. The first of these was a series of nerves that penetrated the capsule wall individually and entered a lamella from the top (Figs 5a–c, 6), dividing at least once within the area of the lamina propria (Fig. 5c) before terminating in finer processes. These fine processes reached the distal portions of the olfactory lamellae, where the candidate magnetoreceptor cells were most often found. One of these fine processes within the lamina propria consistently wrapped around the artery that loops through each olfactory lamella (Fig. 4c). The second branching pattern appeared to arise from a nerve that penetrated the capsule from the base. Successive CLSM optical slices showed that this nerve branched and penetrated several olfactory lamellae from their bases (Fig. 5d). None of the fine processes from either pattern were seen to penetrate the basal lamina or enter the olfactory mucosal layer itself. This dual innervation pattern was subsequently traced in five separate fish.

We can now propose a link from the candidate magnetoreceptor cells in the lamina propria of the olfactory lamellae through the ros V to the brain, summarized in Fig. 6. Our work also revealed a complex and previously undescribed network of ros V fine processes around the olfactory capsule. The function of this network is unknown, but its size, complexity and innervation of the olfactory lamellae invite further investigation.

Implications for magnetoreception

We suggest that vertebrates detect magnetic fields using magnetite-based magnetoreceptors located in the lamina propria of the olfactory epithelium and linked to the brain via the ros V. The presence of both behavioural and electrophysiological responses to magnetic intensity in the trout and the close association between the magnetically responsive nerve and the candidate magnetoreceptor cells indicate that the responses and the candidate receptors are

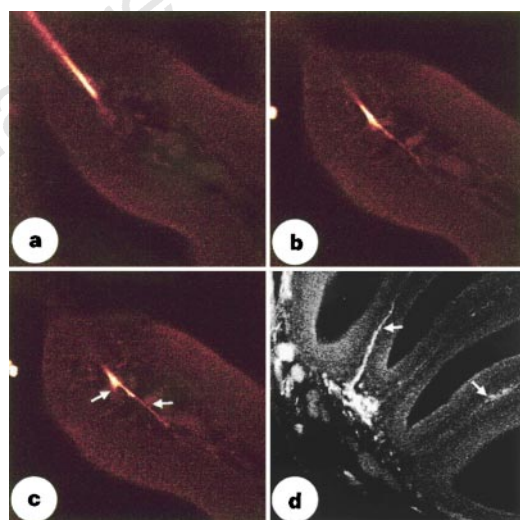


Figure 5 Optical slices showing two different branching patterns of Dil-labelled nerve processes entering trout olfactory lamellae. **a–c**, Three optical slices through a single olfactory lamella (magnification $\times 135$). A labelled fine process from a branch of the ros V can be seen entering the lamella through the top (**a**) and forming two fine processes (in **b**, $22\ \mu\text{m}$ from **a** and in **c**, $27\ \mu\text{m}$ from **a**; arrows). **d**, Fine processes can also be seen entering the lamina propria of several lamellae (arrows) from their bases (magnification $\times 55$). These processes originate from a different branch of the ros V than the one that innervates the top area in **a–c**.

likely to be functionally linked. Robust responses to changes in magnetic field intensity have now been demonstrated behaviourally in fish¹⁸ and turtles⁷, and electrophysiologically in the ros V of fish and in the trigeminal system of birds²⁶. Our reconstructions clearly show that fine processes of the ros V terminate in the region (within the lamina propria of the olfactory lamellae) where the candidate magnetoreceptor cells are found (Fig. 6). Abolition of the effects of impulse magnetization on magnetic orientation behaviour^{13,14} by pharmacological blocking of the trigeminal nerve system²⁷ in birds provides complementary evidence linking behavioural responses to candidate magnetite-based magnetoreceptors. Our results thus

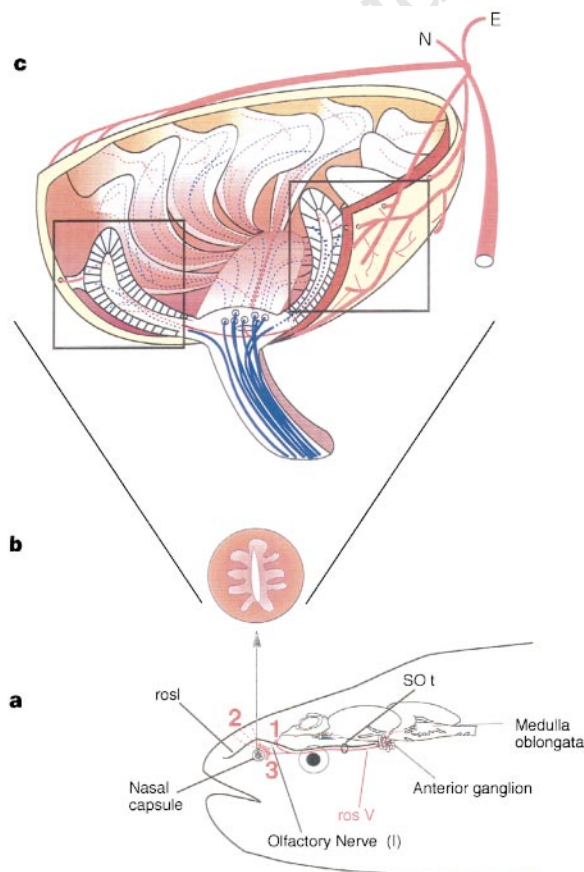


Figure 6 Schematic diagram of the innervation of the head region and nasal capsule of the trout by the SOt branch of the ros V. **a**, Innervation of the SOt (the ros V is shown in red) in the head region of the trout. **b**, Olfactory rosette within the trout nasal capsule (top view). The nasal flap that lies over the top of the olfactory rosette has been removed for clarity. **c**, A three-dimensional diagram of the innervation by the ros V into olfactory lamellae in the nasal capsule of the trout. One process innervates the nasal membrane and flap (N) and the other (top right (E)) is process 2 in **a**. Others form a network of nerves which surround the nasal capsule. Within this network, the smaller branches have fine processes that pass through the nasal membrane lining the nasal capsule and innervate, at both the top and base, individual olfactory lamellae that form the olfactory rosette. The olfactory nerve (blue) is the combination of all axons of the olfactory sensory cells which are situated in the mucosa and send their axons to the olfactory bulb. The network of nerves surrounding the capsule generally lies in a fatty layer (yellow) that is typically found between the neurocranium (not shown) and the outer membrane (brown) that lines the nasal capsule. The pale area in the front two lamellae represents the folded layers of the olfactory epithelium that are separated internally by the lamina propria. New lamellae are formed in the area of the nasal capsule (not shown). The left box outlines the area shown in Fig. 5a–c. The right box outlines the area reconstructed in Fig. 4.

unify results on components of the sense that have been studied separately in a variety of taxa, allowing us to suggest an outline description of the magnetic sense in vertebrates.

Our results suggest that a magnetite-based magnetic sense makes an important contribution to long-distance orientation by animals. Responses to changes in magnetic intensity have been implicated in the formation of a 'magnetic map'^{1,7,26,27}. The behavioural threshold to magnetic intensity changes necessary to form a useful magnetic map can be no more than a few tens of nanotesla (nT). Thresholds of 10–200 nT have been shown experimentally in some birds²⁶ and honeybees²⁸ and inferred for homing pigeons²⁹ and whales^{30,31}. Such sensitivities can only be achieved by averaging the responses of large numbers of magnetite-based magnetoreceptors³².

Location of candidate magnetoreceptors in the nose of the trout also has implications for experiments on long-distance orientation in species such as homing pigeons. The apparent physical proximity of magnetoreception and olfaction raises the intriguing possibility that olfactory impairment would also produce magnetic impairment and so might disrupt long-distance orientation, as seems to occur in homing pigeons^{33–35}. Attaching magnets close to the nose could be expected to disrupt magnetic but not olfactory contributions to homing. Our work thus brings a new perspective to the study of magnetic orientation and provides experimental support for the intuitively appealing hypothesis that animals use the magnetic sense for navigation. □

Methods

Discrimination training. Our procedure¹⁶ differed from that in ref. 18 only as required for working with trout. Fish were trained every second day. Trials lasted 15 s and were separated by a variable intertrial interval (average length 2 min) during which the tank was darkened. In S+ (reinforced stimulus) trials, the first response after 15 s brought food. In S– (non-reinforced stimulus) trials, a penalty timer started after 15 s and was reset by each subsequent response until either it 'timed-out' or a total of 60 s of penalty time had accumulated. To control for possible generalized effects of the experimental field on behaviour³⁶, for one fish, the altered field became the reinforced stimulus (S+) and the uniform background field became the non-reinforced stimulus (S–). For the other two fish, S+ and S– were the background and altered fields, respectively.

Electrophysiological recording. Fish were prepared using standard procedures. Extracellular recordings (using glass microelectrodes filled with 4 M NaCl solution and a silver wire reference electrode) of the activity of single units were made from the ros V where it crosses the top of the orbit. Standard electrophysiological apparatus was used to amplify, record and analyse the activity of units.

The earth plate on which the preparation and apparatus were mounted cancelled the vertical component leaving only the horizontal component (~25 μT) of the Earth's magnetic field present in the experimental tank. Horizontal coils placed on either side of the head of the fish and aligned parallel to the residual background field could be energized to produce fields aligned either parallel or antiparallel to the background field. Potential mechanical artefacts caused by switching of the current to the coils were minimized by the alignment of the coils relative to the background field and by use of rubber insulation to isolate the preparation from the rest of the apparatus.

Intracellular magnetite. Intracellular magnetite was detected using reflectance-mode CLSM. Magnetotactic bacteria were used to validate the detection procedure (Fig. 3a), with *E. coli* as negative controls. For trout olfactory epithelium, tissue was embedded in JB4 resin for viewing in reflectance mode (Fig. 3b). For TEM, the olfactory epithelium was embedded in Epon resin and thin sections taken through a reflection to locate the crystal shown in Fig. 3c,d (inset) Figure 3d shows the results of energy dispersive analysis of X-ray emissions of the area of the section immediately surrounding the crystal.

Nerve tracing and three-dimensional reconstruction. Juvenile trout (40–60 mm) were anaesthetized in 0.05% MS 222, measured and decapitated just behind the gill cover. After immersion in fixative for 24 h, DiI crystals were applied to the exposed ros V on one side, the head immersed in fresh fixative and placed in an incubator at 37 °C for up to 25 days.

Optical slices in 2-μm steps were taken through four 100-μm gelatin sections using a Leica TCS 4D confocal laser scanning microscope. For three-dimensional reconstruction, the images were cut and pasted using NIH Image into a 512 × 512 format with the 256 × 256 pixel image centrally located, allowing subsequent alignment of laterally offset data sets. Images were combined by selecting fiducial points and realigning all subsequent optical slices within each data set to form a single 149-image three-dimensional data stack (446 μm wide × 685 μm × 298 μm deep). Three-dimensional reconstruction was done using VoxelView software (Vital Images, Fairfield, Iowa). Rotation of the reconstruction enabled finely detailed tracking of the rami of the ros V entering the olfactory lamellae.

Received 29 August 1996; accepted 17 September 1997.

1. Wiltschko, R. & Wiltschko, W. *Magnetic Orientation in Animals* (Springer, Berlin, 1995).
2. Leask, M. J. M. A physicochemical mechanism for magnetic field detection by migratory birds and homing pigeons. *Nature* **267**, 144–145 (1977).
3. Phillips, J. B. & Borland, S. C. Behavioural evidence for use of a light-dependent magnetoreception mechanism in a vertebrate. *Nature* **359**, 142–144 (1992).
4. Kalmijn, A. J. Biophysics of geomagnetic field detection. *IEEE Trans. Magn.* **17**, 1113–1124 (1981).
5. Gould, J. L., Kirschvink, J. L. & Deffeyes, K. D. Bees have magnetic remanence. *Science* **201**, 1026–1028 (1978).
6. Walcott, C., Gould, J. L. & Kirschvink, J. L. Pigeons have magnets. *Science* **205**, 1027–1029 (1979).
7. Lohmann, K. J. & Lohmann, C. M. F. Detection of magnetic field intensity by sea turtles. *Nature* **380**, 59–61 (1996).
8. Quinn, T. P., Merrill, R. T. & Brannon, E. L. Magnetic field detection in sockeye salmon. *J. Exp. Zool.* **217**, 137–142 (1981).
9. Lohmann, K. J. *et al.* Magnetic orientation of spiny lobsters in the ocean: Experiments with undersea coil systems. *J. Exp. Biol.* **198**, 2041–2048 (1995).
10. Kirschvink, J. L. & Gould, J. L. Biogenic magnetite as a basis for magnetic field detection in animals. *Biosystems* **13**, 181–201 (1981).
11. Yorke, E. D. A possible magnetic transducer in birds. *J. Theor. Biol.* **89**, 533–537 (1979).
12. Walker, M. M. & Bitterman, M. E. Attached magnets disrupt magnetic field discrimination by honeybees. *J. Exp. Biol.* **141**, 447–451 (1989).
13. Wiltschko, W., Munro, U., Beason, R. C., Ford, H. & Wiltschko, R. A magnetic pulse leads to a temporary deflection in the orientation of migratory birds. *Experientia* **50**, 697–700 (1994).
14. Beason, R. C., Dussourd, N. & Deutschlander, M. E. Behavioural evidence for the use of magnetic material in magnetoreception by a migratory bird. *J. Exp. Biol.* **198**, 141–146 (1995).
15. Kreithen, M. L. & Keeton, W. T. Attempts to condition homing pigeons to magnetic stimuli. *J. Comp. Physiol. A* **91**, 355–362 (1974).
16. Woodard, W. T. & Bitterman, M. E. A discrete trials/fixed-interval method of discrimination training. *Behav. Res. Meth. Instr.* **6**, 389–392 (1974).
17. Mann, S., Sparks, N. H. C., Walker, M. M. & Kirschvink, J. L. Ultrastructure, morphology and organization of biogenic magnetite from sockeye salmon, *Oncorhynchus nerka*: Implications for magnetoreception. *J. Exp. Biol.* **140**, 35–49 (1988).
18. Walker, M. M. Learned magnetic field discrimination in the yellowfin tuna, *Thunnus albacares*. *J. Comp. Physiol. A* **155**, 673–679 (1984).
19. Walker, M. M. & Bitterman, M. E. Conditioned responding to magnetic fields by honeybees. *J. Comp. Physiol. A* **157**, 67–71 (1985).
20. Walker, M. M., Baird, D. L. & Bitterman, M. E. Failure of stationary but not of flying honeybees to respond to magnetic field stimuli. *J. Comp. Psychol.* **103**, 62–69 (1989).
21. Carman, G. J., Walker, M. M. & Lee, A. K. Attempts to demonstrate magnetic discrimination by homing pigeons in flight. *Anim. Learn. Behav.* **15**, 124–129 (1987).
22. Kirschvink, J. L. Magnetite biomineralization and geomagnetic sensitivity in animals: An update and recommendations for future study. *Bioelectromagnetics* **10**, 239–259 (1989).
23. Moore, A., Freake, S. M. & Thomas, I. M. Magnetic particles in the lateral line of the Atlantic salmon (*Salmo salar* L.). *Phil. Trans. R. Soc. Lond. B* **329**, 11–15 (1990).
24. Puzdrowski, R. L. Afferent projections of the trigeminal nerve in the goldfish, *Carassius auratus*. *J. Morphol.* **198**, 131–147 (1988).
25. Blakemore, R. P. Magnetotactic bacteria. *Science* **190**, 377–379 (1975).
26. Semm, P. & Beason, R. C. Responses to small magnetic field variations by the trigeminal system of the bobolink. *Brain Res. Bull.* **25**, 735–740 (1990).
27. Beason, R. C. & Semm, P. Does the avian ophthalmic nerve carry magnetic navigational information? *J. Exp. Biol.* **199**, 1241–1244 (1996).
28. Walker, M. M. & Bitterman, M. E. Honeybees can be trained to respond to very small changes in geomagnetic field intensity. *J. Exp. Biol.* **145**, 489–494 (1989).
29. Walcott, C. Magnetic orientation in homing pigeons. *IEEE Trans. Magn.* **Mag-16**, 1008–1013 (1980).
30. Kirschvink, J. L., Dizon, A. E. & Westphal, J. A. Evidence from strandings for geomagnetic sensitivity in cetaceans. *J. Exp. Biol.* **120**, 1–24 (1986).
31. Walker, M. M., Kirschvink, J. L., Ahmed, G. & Dizon, A. E. Fin whales (*Balaenoptera physalus*) avoid geomagnetic gradients during migration. *J. Exp. Biol.* **171**, 67–78 (1992).
32. Kirschvink, J. L. & Walker, M. M. in *Magnetite Biomineralization and Magnetoreception by Living Organisms: A New Biomagnetism* (eds Kirschvink, J. L., Jones, D. S. & MacFadden, B. J.) 243–254 (Plenum, New York, 1985).
33. Benvenuti, S. & Walraff, H. G. Pigeon navigation: site simulation by means of atmospheric odours. *J. Comp. Physiol. A* **156**, 737–746 (1985).
34. Papi, F. Pigeons use olfactory cues to navigate. *Ethol. Ecol. Evol.* **1**, 219–231 (1989).
35. Walraff, H. G. Relevance of atmospheric odours and geomagnetic field to pigeon navigation: what is the "map" basis? *Comp. Biochem. Physiol. A* **76**, 643–663 (1983).
36. Sidman, M. *Tactics of Scientific Research: Evaluating Experimental Data in Psychology*. (Basic Books, New York, 1960).
37. Moench, T. T. & Konetzka, W. A. A novel method for the isolation and study of a magnetotactic bacterium. *Arch. Microbiol.* **119**, 203–212 (1978).

Acknowledgements. We thank the Whitehall Foundation, Marsden Fund, New Zealand Lotteries Grants Board, Auckland University Research Committee and School of Biological Sciences for support; W. T. M. Grijters, B. M. Davy, I. MacDonald, V. Ward, A. Young and A. Cantell for technical assistance; and M. E. Bitterman, A. R. Bellamy and G. G. Dodson for helpful comments on earlier drafts of the manuscript.

Correspondence and requests for materials should be addressed to M.M.W. (e-mail: m.walker@auckland.ac.nz).